scientific reports

Check for updates

OPEN

Two new *Caymanostella* species discovered at deep-sea wood falls in the Clarion Clipperton Fracture Zone

Magdalini Christodoulou[1]✉, Christopher Mah[2] & Pedro Martinez Arbizu[3]

In an era where human activities increasingly impact the deep sea and, with future ventures such as deep-sea mining on the horizon, describing deep-sea biodiversity is vital for conservation, sustainable resource management, understanding global ecological processes, and informing policy decisions. Polymetallic nodule fields, in particular, have been proven to be reservoirs of previously undiscovered biodiversity. As part of ongoing efforts to unveil this dark diversity, two new species of *Caymanostella* –*Caymanostella persephone* nov. sp. and *Caymanostella hades* nov. sp.,– recovered on a single piece of sunken wood in the Clarion Clipperton Fracture Zone, a region in the eastern Pacific Ocean targeted for mining, are described herein. Although both species were sampled on the same piece of wood, they are genetically distinct and can be differentiated from each other and their congeners morphologically by various morphological characters, including the arrangement of the central plates, the position of gonopores, and the form of their abactinal armaments. The discovery of the new species brings the total number within the *Caymanostella* genus to ten and expands the known geographical distribution of the genus.

Keywords Sea stars, Mining, Polymetallic nodule fields, Deep sea, Echinodermata

The worldwide increase in demand for metals such as manganese, cobalt, and nickel has sparked unprecedented attention towards deep-sea environments rich in mineral deposits[1–3]. The Clarion-Clipperton Fracture Zone (CCFZ), in the equatorial Pacific Ocean, attracts significant attention from the mining industry because of its vast nodule deposits rich in critical metals thought to surpass the entire terrestrial reserve base[3–5]. Covering approximately six million km^2, this area features depths of 4,000 to 6,000 m with an abyssal plain seafloor blanketed with sediment and rich in potato-sized polymetallic nodules engulfing metals critical to the industry. This region lies within areas beyond national jurisdiction (ABNJ), legally designated under the United Nations Convention on the Law of the Sea (UNCLOS) and falls under the regulation of the International Seabed Authority (ISA)[6]. To effectively manage the potential environmental impacts of deep-sea mining activities, it is critical to have a comprehensive understanding of the area's biodiversity before (and if) any large-scale mining operations commence. However, until recently, this fundamental knowledge was severely lacking. The technological advancements coupled with the interest in deep-sea mining have allowed a dramatic increase in our ability to explore and sample this area. Thus, beyond its mineral wealth, recent studies have shown that CCFZ is also a vital reservoir of biodiversity, hosting a wide array of life forms adapted to its extreme conditions[7–9]. The biodiversity of this area is thought to be largely undiscovered, with recent studies revealing numerous previously undescribed species[9–11]. The existence of these yet-to-be-discovered species presents substantial obstacles to accurately assessing the biodiversity of the CCFZ[9]. This situation emphasizes the critical importance of ongoing scientific exploration and thoughtful analysis of potential consequences as interest in deep-sea mining continues to escalate. As we stand on the brink of potentially transformative industrial activities in these depths, the role of the scientific community in uncovering and cataloging this unknown life becomes increasingly crucial for informed decision-making and sustainable management of these unique marine habitats.

[1]Biodiversity Center Upper Austria, OÖ Landes-Kultur GmbH, Johann- Wilhelm-Klein-Straße 73, 4040 Linz, Austria. [2]Department of Invertebrate Zoology, National Museum of Natural History, Smithsonian Institution, 10th and Constitution Avenue NW, 20560 Washington, D.C, USA. [3]Senckenberg am Meer, German Centre for Marine Biodiversity Research (DZMB), Südstrand 44, 26382 Wilhelmshaven, Germany. ✉email: Magdalini.Christodoulou@ooelkg.at

Benthic megafauna (organisms > 10 mm) inhabiting the seafloor, have been prioritised for monitoring deep-sea ecosystems due to their ability to be observed and processed through seabed imagery, providing insights into food web dynamics, ecosystem functioning, and the impacts of disturbances and subsequent recovery processes[12–14]. In the CCFZ, megafaunal organisms have been surveyed almost exclusively from video and photographic data[12,13,15–17]. While image-based surveys have significantly advanced our knowledge of CCFZ's biodiversity, they have limitations. The primary challenge lies in accurately identifying the morphotypes observed in these images and determining whether they correspond to known species or to new yet-to-be described species[18]. To address this issue, it is essential to combine the visual surveys with physical sampling, leading to precise species identification which in turn will allow to assess the uniqueness of the CCFZ fauna and its degree of connectivity to other deep-sea ecosystems, crucial for effective conservation and management strategies at the onset of potential deep-sea mining[18].

Among the megafaunal taxa collected in the CCFZ, Echinodermata are one of the most widespread and abundant[11,15]however, little is known about the sea stars (Asteroidea) occurring in CCFZ. Asteroids are found in all the oceans of the world, from the shallow waters to the deep sea, numbering over 1900 extant species[19]. Out of the 36 families of living Asteroidea, 15 occur exclusively in deep-sea habitats, and 14 families have deep-sea members[19].

Caymanostellidae is a remarkable group of morphologically unique sea stars that are rarely encountered and more seldom collected that have exclusively been associated with wood falls in the deep sea[20–22]. They are a small-sized family with a pentagonal/subpentagonal to stellate body shape, and a set of unique characters (i.e. abactinal placement of the superomarginal plates, presence of five actinal chambers inter-radially on the oral side, bar-shaped adambulacral plates, absence of actinal plates) that distinguish them from other asteroid families[20–22]. The family currently comprises two genera (*Belyaevostella* Rowe, 1989 and *Caymanostella* Belyaev, 1974) after Shen and collaborators[22] placed the genus *Crinitostella*[23] as a junior synonym of *Caymanostella*. Caymanostellidae comprises 10 species (*Belyaevostella*: 2 species; *Caymanostella*: 8 species) in total, demonstrating a distribution across the world's major Oceans, Atlantic, Pacific and Indian, and an extensive bathymetric range between ~ 414 and 6780 m[21,22]. The first recorded *Caymanostella* species, *C. spinimarginata* Belyaev, 1974 was described from the Caribbean Sea (Cayman Trench), whereas the rest nine species, *C. admiranda* Belyaev & Litvinova, 1977, *C. phorcynis* Rowe, 1989, *C. madagascarensis* Belyaev & Litvinova, 1991, *C. laguardai* (Martin-Cao-Romero et al., 2021), *C. davidalani* Shen et al. 2024, *C. loresae* Shen et al. 2024, and *C. scrippscognaticausa* Shen et al. 2024, were described from the West Indian and the Southeast Pacific Oceans. Finally, Dilman et al.[21] collected three *Caymanostella* specimens from the Kuril-Kamchatka Trench area (off Japan) with similar morphology to *C. spinimarginata* which they opted to identify as *C.* cf. *spinimarginata* despite the large geographical distance from the type locality of *C. spinimarginata*. As no genetic information is currently available for the *C. spinimarginata* from its type locality, the species assignment is pending. An expedition to the Clarion Clipperton Fracture Zone has resulted in the observation of many *Caymanostella* specimens and the actual collection of two specimens that each represent a new species of *Caymanostella*. Molecular and morphological data are employed to support the validity of these two new caymanostellid sea stars.

Results

Systematics

Family Caymanostellidae Belyaev, 1974

Genus *Caymanostella* Belyaev, 1974.

***Caymanostella persephone* nov. sp.**

(Figs. 1A–E, 2A–E, 3A–E, 3I, 3J, 3M, 3N)

urn: lsid: zoobank.org: act:01 A2 A1E2-AEDF-4555-9 A0B-98 CABE18BD2 C.

Diagnosis. Body subpentagonal. Abactinal plates fan-shaped to polygonal, imbricating. Dense and granuliform abactinal armaments. Large granules with a wide base and a conical-shaped crown, featuring large, multi-tipped, prong-like structures. Gonopores visible, piercing the proximal-most superomarginal plates. Madreporite with branching grooves. One row of dorsolateral plates on each side of a row of carinal plates extending to arm tip. Terminal plate rectangular. Inferomarginal plates more elongate than adjoining superomarginal. Adambulacral spines oblong with a club-shaped base, devoid of jagged tips near base and serrated tips.

Material examined. Holotype: 1 ind. SMF 6947, (field ID: SO239-161-1), RV SONNE, cruise SO239 EcoResponse, Clarion and the Clipperton Fracture Zone, (IFREMER licence area) St.161, 15.04.2015, 14° 2.07' N, 130° 5.60' W, depth 5030.7 m, on sunken wood fall together with *C. hades* nov. sp., Arbaciidae sp., and *Munidopsis* sp.

Holotype Description. Adult. Size: $R = 9$ mm, $r = 8.5$ mm (specimen is uplifted and bent on one side). Five rays, body form subpentagonal (Figs. 1A and B and 2A and E). The abactinal surface is covered with imbricating fan- to polygonal- shaped plates similar in size, with the five primary inter-radial plates being the largest. Also distinguishable are the five fan-shaped plates, between the proximal-most superomarginal plates on each arm (Figs. 1A and 2A, B, C and D). One of the primary inter-radial plates bears a madreporite, which has the appearance of several branching grooves and covered by nine large plate-shaped granules (Fig. 2B and C). A row of carinal plates stretches in each arm with a row of dorsal-lateral plates on each side of the carinal row; rows of plates become less clear closer to the central disc (Figs. 1A and 2A, B, C and D). At the tip of each arm, there is a rectangular-shaped terminal plate with a central opening (pore). Marginal plates are arranged in two parallel rows along the body margin, peripheral to the abactinal plates; these plates are elongated and oriented perpendicularly or slightly obliquely to the body margin; there are 13 superomarginal and 13 inferomarginal plates along each side of the arm decreasing in size towards the arm tip; the distal-most superomarginal plates are conspicuously larger in size compared with the next adjacent plates and have piercing gonopores towards the upper margins (Fig. 2A and D). Gonopores are covered by six plate-shaped spinelets (Fig. 1A, C and D). On the

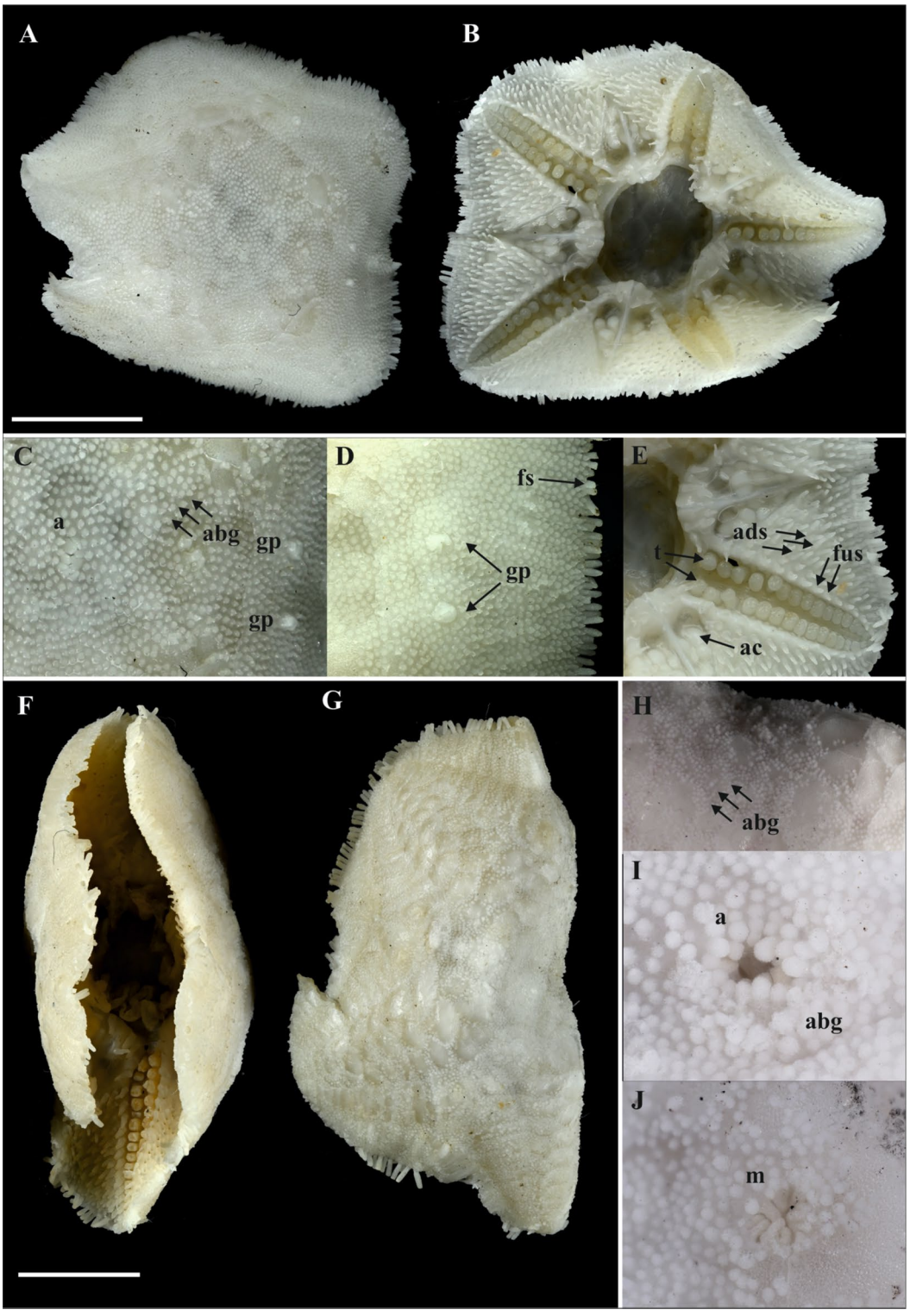

Fig. 1. *Caymanostella persephone* nov. sp., Holotype (SMF 6947): **A**, abactinal surface; **B**, actinal surface; **C**, close up of abactinal surface; **D**, close up of gonopores and marginal surface; **E**, close up of actinal surface. *Caymanostella hades* nov. sp., Holotype (SMF 6948): **F**, actinal surface; **G**, abactinal surface; **H**, close up of abactinal surface; **I**, anus; **L**, madreporite. Scale bars: 1 cm. a, anus; abg, abactinal granules; ac, actinal chamber; ads, adambulacral spines; fs, fringe spines; fus, furrow spines; gp, gonopore; t, tube foot; m, madreporite.

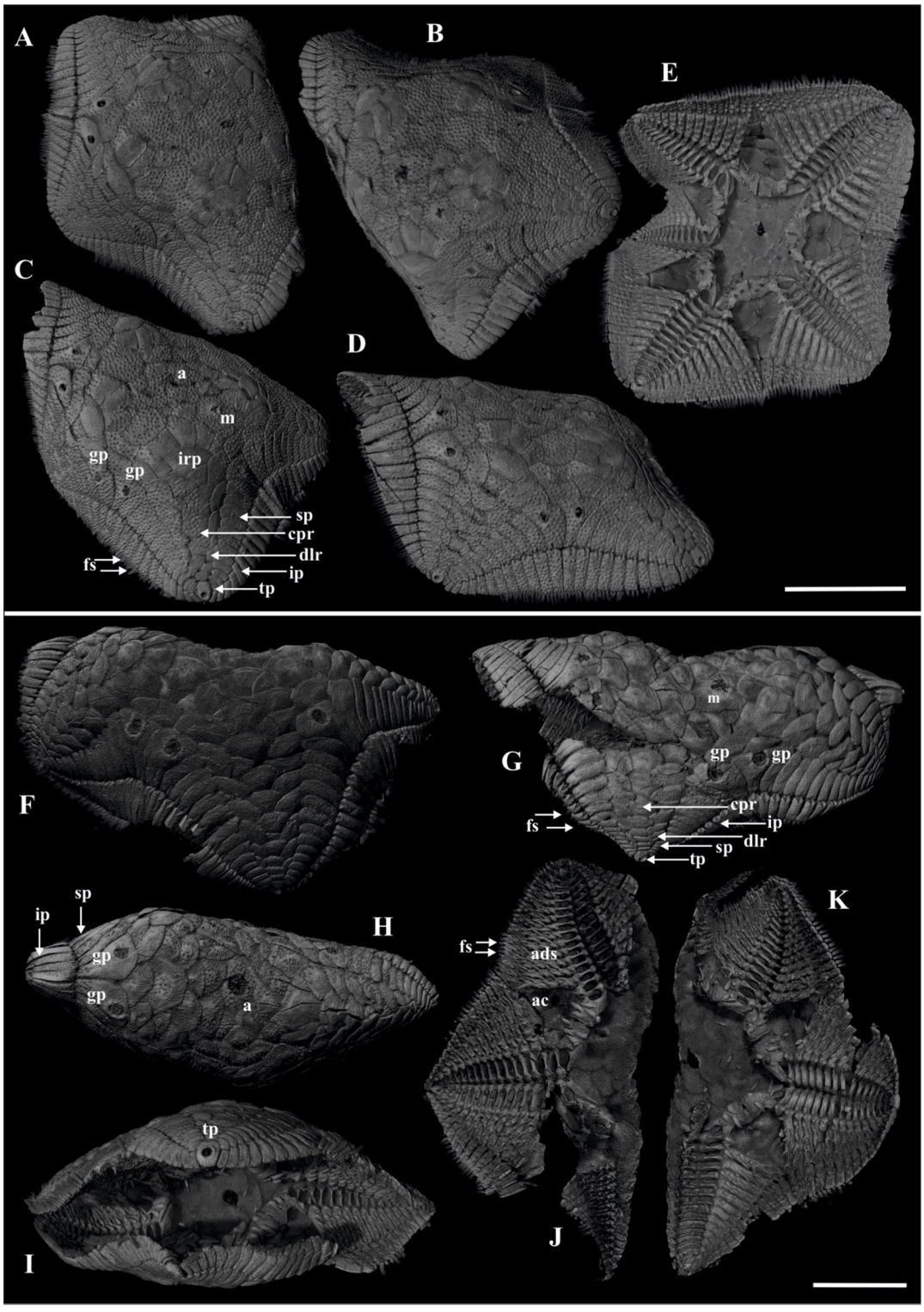

Fig. 2. MicroCT images of *Caymanostella persephone* nov. sp., Holotype (SMF 6947) and *Caymanostella hades* nov. sp., Holotype (SMF 6948): A–D, abactinal surface *C. persephone*; E, actinal surface of *C. persephone*. F–H, abactinal surface *C. hades*; I–K, actinal surface of *C. hades*. Scale bars: 1 cm. a, anus; ac, actinal chamber; ads, adambulacral spines; crp, central row plates; dlr, dorsal-lateral plates; fs, fringe spines; fus, furrow spines; gp, gonopore; ip, inferomarginal plates; irp, inter-radial plates; m, madreporite; sp, superomarginal plates; tp, terminal plate.

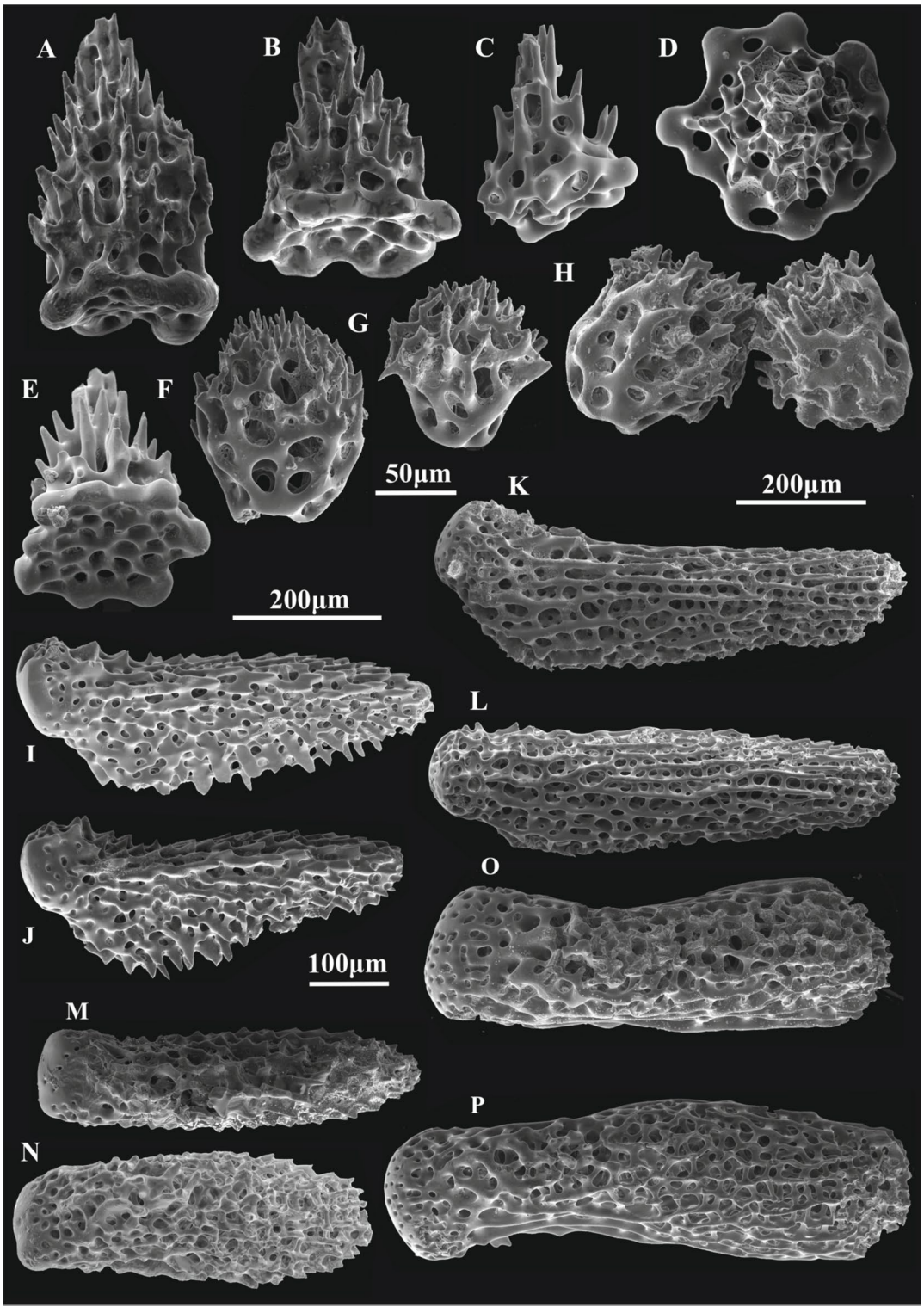

Fig. 3. Scanning Electron Microscopy (SEM) images of spines of *Caymanostella persephone* nov. sp., Holotype (SMF 6947) and *Caymanostella hades* nov. sp., Holotype (SMF 6948): A–E, abactinal granules of *C. persephone;* F–H, abactinal granules of *C. hades*; I–J, inferomarginal spines of *C. persephone;* K–L, inferomarginal spines of *C. hades;* M–N, actinal spines *C. persephone*; O–P, actinal spines *C. hades*. Scale bars: A–H, 50 µm, I–L, 200 µm; M–P, 100 µm.

terminal end of each inferomarginal plate are two (in smaller plates at tip of arm) to three elongated fringe spines (rarely four) (Figs. 1A and D and 2C and D). The fringe (marginal) spines are 0.53–0.57 mm long, with a club-shaped basis and a wing-shaped body with serrate edges (Fig. 3I and J). Armature of abactinal, superomarginal plates and inferomarginal plates (abactinal side) is composed of uniform conical granules, however larger granules are found around the madreporite and gonopores (Fig. 1C and D). Central disc plates can bear 30 to 50 granules, superomarginal plates bear 10 to 45, and inferomarginal plates bear 9 to 35 (Fig. 1A, C and D). On marginal plates, abactinal granules tend to arrange in rows (2–4 rows) (Fig. 2A, B, C and D). Granules are composed of multi-tipped prong-like support structures around central axis, each prong with multiple jagged tips distributed on different levels and wide perforated bases, round to polygonal in outline varying between 0.13 and 0.21 mm in size (Fig. 3A, B, C, D and E). Ambulacral furrows are narrow and petaloid in shape (Figs. 1B and 2E). There are 14 pairs of adambulacral elongated and bar-like plates in each arm (except proximal-most and distal-most plate which are much smaller and not elongated) extending from the furrow to the inferomarginal plates; the first adambulacral plate is the shortest and borders the actinal chamber, whereas the second plate extends alongside the chamber; the second and third plates are the longest; the subsequent plates decrease in size towards the arm tip (Figs. 1B and E and 2E). Adambulacral plates and the oral sides of the inferomarginal plates are uniformly covered by tapering, serrate spines (Fig. 3M and N). Adambulacral plates bear up to 11 spines (one spine on the first, shortest plate). Each plate bears one furrow spine (not counted with the 11). The second spine is usually placed further from the furrow, and the subsequent spines are arranged across the plate in two alternating rows (Fig. 1B and E). Adambulacral spines are 0.44–0.50 mm long, finely serrated, oblong with a club-shaped basis; spines are devoid of jagged tips near base while tips are serrated (Fig. 3M and N). Five heart-shaped actinal chambers covered by a thin semi-transparent membrane occur inter-radially on the oral side, one in each inter-radius; each actinal chamber is separated into two parts by a septum. Five to eight oval gonad lobes (approximately 0.87 × 0.77 mm), are visible inside some of the chambers through the actinal membrane (Figs. 1B and 2E). The oral opening is large, and star shaped, 7.9 mm long and 6.5 mm wide (Figs. 1B and 2E). Paired oral plates are broader than long, without a median keel. Each plate bears two marginal spines, situated on the oral edge and at the corner, and two suboral spines. Suckered tube feet are in two rows, 15 pairs along each arm (Figs. 1B and 2E).

Etymology. Named after the Greek mythological goddess and queen of the dark underworld, Persephone, wife of Hades, akin to the habitat of the new asteroid species; used as a noun in apposition.

Type locality. Clarion Clipperton Fracture Zone (IFREMER licence area), Eastern Pacific Ocean.

Distribution. Known only from the type locality (Fig. 4).

Habitat. The new species was collected from a wood fall among polymetallic fields in the Clarion Clipperton Fracture Zone (Fig. 5). The specimen was collected with ROV *Kiel 6000* at 5030.7 m deep.

Colour pattern. Body colour in life is white (Fig. 5).

Remarks: The subpentagonal body shape of the new species, *C. persephone* nov. sp., can be easily distinguished from *C. scrippscognaticausa* and *C. laguardai* having stellate body type (Fig. 1A vs. Shen et al.[22] Fig. 5A and Martin-Cao-Romero et al.[23] Fig. 1). Likewise stellate body although less pronounced is observed in *C. phorcynis* (Fig. 6) and *C. davidalani* (Shen et al.[22] Fig. 11 C). The position of the gonopores (piercing the two

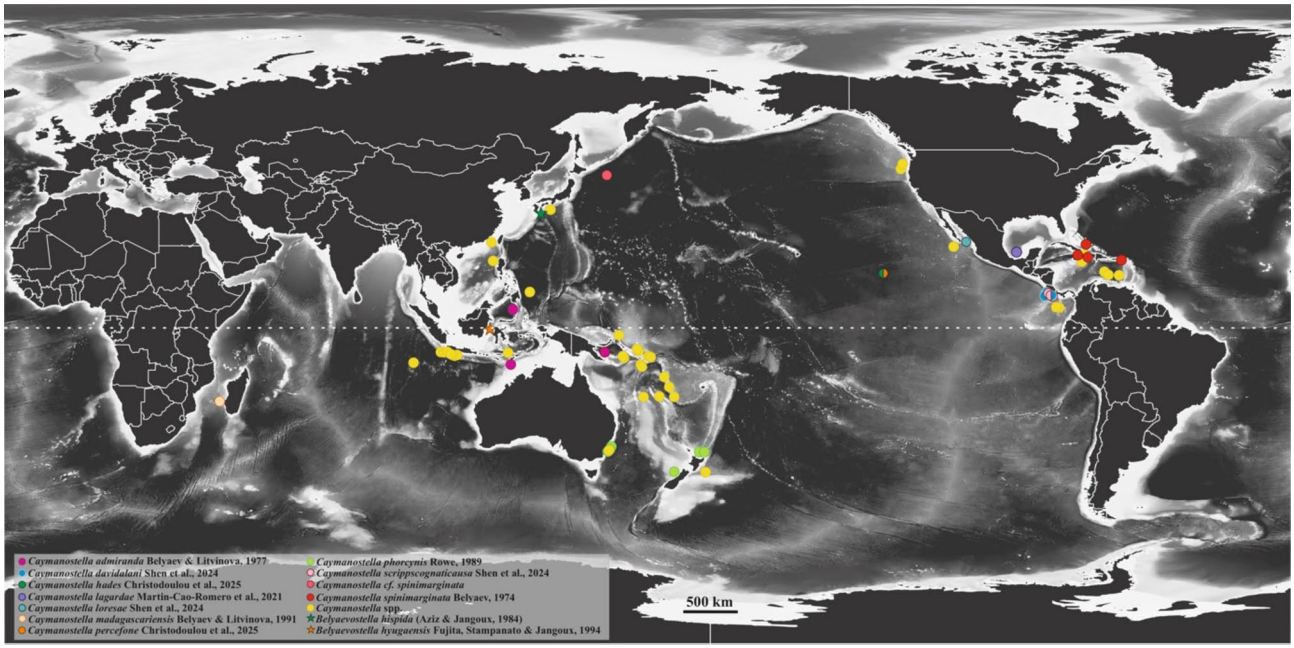

Fig. 4. Distribution of *Caymanostella* species, including the sampling location of newly described species. Detailed information on the distribution records is provided in Supplementary Table S1. Made with Natural Earth. Free vector and raster map data @ naturalearthdata.com.

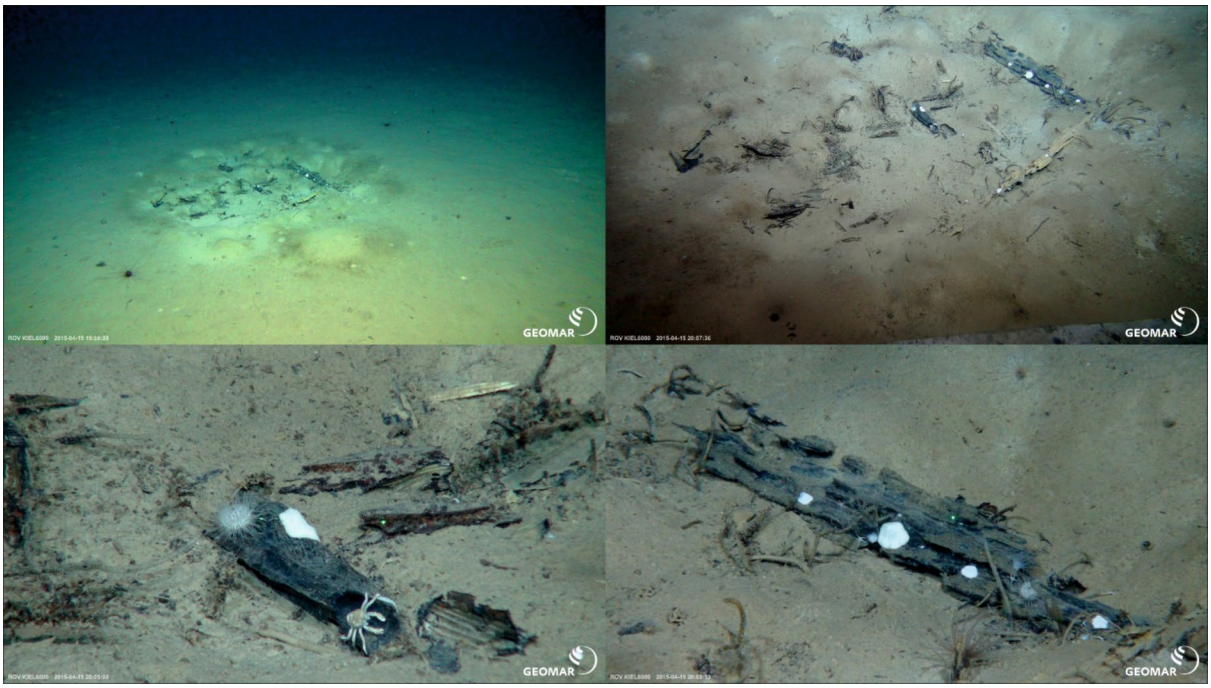

Fig. 5. Collection site (wood falls) of new species found during the SO239 cruise in the IFREMER-East exploration licence area. New species were found attached to the smaller wood piece (down left). Photos by ROV *KIEL 6000* Team/GEOMAR Kiel.

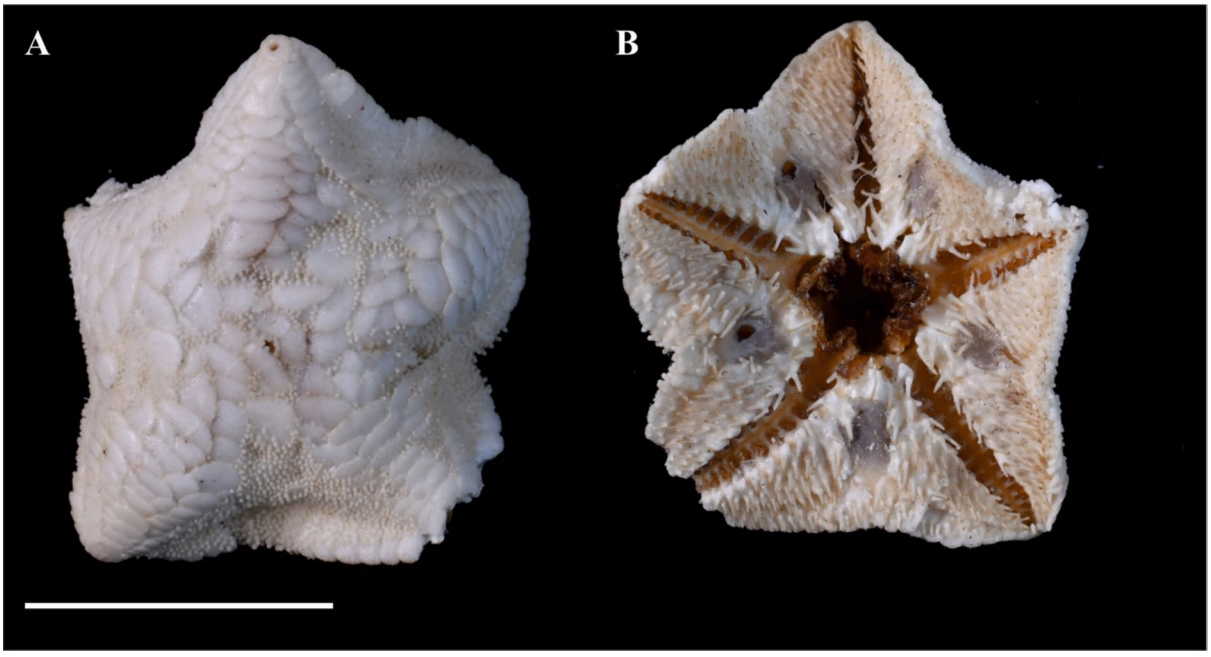

Fig. 6. *Caymanostella phorcynis* Rowe, 1984. Holotype (AM J18911): A, abactinal surface; B, actinal surface. Scale: 0.5 cm. Photo courtesy of the Australian Museum by A. Hugedus.

proximal-most superomarginal plates) separates the new species from *C. davidalani*, *C. scrippscognaticausa*, *C. spinimarginata* and *C.* cf. *spinimarginata* having gonopores in notches on the proximal margins of two proximal-most superomarginal plates (Fig. 2A, B, C and D vs. Shen et al.[22]: *C. davidalani*: Fig. 3B; *C. scrippscognaticausa*: Fig. 8B; Dilman et al.[21]: *C. spinimarginata*: Fig. 2E; *C.* cf. *spinimarginata*: Fig. 2G). The granuliform abactinal armament of the new species distinguishes it from *C. davidalani*, *C. laguardai*, *C. scrippscognaticausa*, and *C. spinimarginata* (including *C.* cf. *spinimarginata*) having spiniform abactinal armament. The new species,

C. persephone armament is similar to *C. admiranda*, *C. hades*, *C. madagascarensis*, and *C. loresae* in being granuliform. However, under high magnification, granules of *C. persephone* have a wide base with a conical-shaped crown featuring large, less dense, multi-tipped prong-like structures and they are large in size (Fig. 3A, B, C, D and E vs. dome-shaped in *C. admiranda*: Dilman et al.[21], Fig. 6A and B; *C. lorsae*: Shen et al.[22], Fig. 16E, 16 F; and *C. hades*, Fig. 4F and G, and spherical pierced with holes in C. *madagascarensis* (Dilman et al.[21], Fig. 6D and E). The two new species can be further discriminated by the terminal plate being more elongated in *C. persephone* (Fig. 2C and D) than in *C. hades* (Fig. 2I). Finally, the mean genetic distances (p-distance) between the new species and its congeneric species were significantly high, ranging from 13.3 to 18.2% for COI and 9.5–13.6% for 16S (Table 1).

***Caymanostella hades* nov. sp.**

(Figs. 1F–J, 2F–K, 3F–H, 3K, 3L, 3O, 3P)

urn: lsid: zoobank.org: act:296D9 CF4-EDB4-47E2-9 A47-576 FCBF656DF.

Diagnosis. Body subpentagonal. Abactinal plates imbricating, fan-shaped and similar in size. Dense and granuliform abactinal armament. Granules dome-shaped, composed of small multi-tipped prong-like support structures with narrow perforated bases. Gonopores visible, piercing the proximal-most superomarginal plates. Madreporite with branching grooves. One row of dorsal-lateral plates on each side of one row of carinal plates until arm tip. Terminal plate square-shaped. Inferomarginals slightly more elongate than adjoining superomarginals. Adambulacral spines oblong, with a club-shaped base, devoid of jagged tips near base and subtle serrated tips.

Material examined: Holotype: 1 ind. SMF 6948, (field ID: SO239-161-2), RV SONNE, cruise SO239 EcoResponse, Clarion and the Clipperton Fracture Zone, (IFREMER licence area) St.161, 15.04.2015, 14° 2.07' N, 130° 5.60' W, depth 5030.7 m, on sunken wood fall together with *Caymanostella persephone* nov. sp., Arbaciidae sp., and *Munidopsis* sp.

Holotype Description: Adult. Size: $R = 11.5$ mm, $r = 10$ mm (specimen is folded). Five rays, body form subpentagonal (Figs. 1G and 2F, J and K). The abactinal surface is covered with imbricating fan-shaped plates similar in size, with the five primary inter-radial plates being among the largest (Figs. 1G and 2F, G and H). One of the primary inter-radial plates bears a madreporite, which has the appearance of several branching grooves and is surrounded by granules (Figs. 1J and 2G). A clear row of carinal plates stretches in each arm with a row of dorsal-lateral plates on each side of the carinal row (Fig. 2F and G). At the tip of each arm, there is a square-shaped terminal plate with a central opening (Fig. 2I). Marginal plates are arranged in two parallel rows along the body margin, peripheral to the abactinal plates; these plates are elongated and oriented perpendicularly or slightly obliquely to the body margin; there are 15 superomarginal and 15 inferomarginal plates along each side of the arm decreasing in size towards the arm tip; each inferomarginal plate slightly more elongated compared to adjoining superomarginal plate. the distal-most superomarginal plates are conspicuously larger in size compared with the next adjacent plates and have gonopores piercing towards the upper margins (Fig. 2F, G and H). At the terminal end of each inferomarginal plate, there are two to three elongated fringe spines (Fig. 1F and G). The marginal spines are 0.62–0.64 mm long, scarcely serrated, and subtly wing-shaped with a club-shaped base (Fig. 3K and L). The armature of abactinal, superomarginal plates and inferomarginal plates is uniform and very dense, composed of oval-shaped granules (Fig. 1H and I). Central disc plates can bear 40 to 60 granules, supermarginal plates bear 13 to 85, and inferomarginal plates bear 10 to 45. Granules are dome-shaped, composed of small multi-tipped prong-like support structures around central axis each prong with multiple jagged tips distributed on different levels and thick with narrow, perforated bases, varying between 0.20 and 0.28 mm in size (Fig. 3F, G and H). Ambulacral furrows are narrow and petaloid in shape. There are 15 pairs of adambulacral elongated and bar-like plates in each arm (proximal-most and distal-most plates are much smaller and not elongated) extending from the furrow to the inferomarginal plates (Fig. 2J and K); the first adambulacral plate is the shortest and borders the actinal chamber, whereas the second plate extends alongside the chamber; the second and third plates are the longest; the subsequent plates decrease in size towards the arm tip (Fig. 2J and K). Adambulacral plates and the oral sides of the inferomarginal plates are uniformly covered by tapering, serrate spines (Fig. 3O and P). Adambulacral plates bear up to 12 spines (two spines on the first, shortest plate). Each plate bears one furrow spine. The second spine is usually placed further from the furrow, and the subsequent spines are arranged across the plate in two alternating rows. Adambulacral spines are 0.60–0.67 mm long, oblong-shaped with a club-shaped basis; spines are devoid of jagged tips near the base while

		1	2	3	4	5	6	7	8	9
1	*Caymanostella hades* nov. sp.		10.8%	13.7%	13.5%	13.9%	12.7%	13.7%	14.6%	9.1%
2	*Caymanostela persephone* nov. sp.	16.3%		11.8%	9.5%	12.3%	10.4%	9.5%	13.6%	13.5%
3	*Caymanostella davidalani*	19.2%	18.2%		12.2%	5.6%	6.5%	14.1%	8.6%	14.2%
4	*Caymanostella loresae*	17.3%	13.3%	17.0%		13.1%	11.2%	13.4%	14.6%	15.0
5	*Caymanostella scrippscognaticausa*	19.1%	17.4%	12.0%	18.7%		6.5%	12.8%	6.4%	15.8%
6	*Caymanostella* cf. *spinimarginata*	17.3%	13.5%	15.2%	15.3%	15.5%		11.7%	10.4%	14.1%
7	*Caymanostella* sp. ("*spinimarginata*")	17.8%	16.3%	18.2%	16.0%	18.0%	17.9%		14.1%	15.4%
8	*Caymanostella laguardai*	--	--	--	--	--	--	--		16.8%
9	*Caymanostella* sp.	--	--	--	--	--	--	--	--	

Table 1. Sequence pairwise mean distance (p-distance) for COI (below the diagonal) and 16 S (above the diagonal) gene of *Caymanostella* species.

tips are subtly serrated (Fig. 3O and P). Five heart-shaped actinal chambers covered by a thin, semi-transparent membrane occur inter-radially on the oral side, one in each inter-radius; each actinal chamber is separated into two parts by a septum. The oral opening is large and elongated, 9.0 mm long and 6.4 mm wide (Fig. 2J and K). Paired oral plates are broader than long, without a median keel. Suckered tube feet are in two rows, 16 pairs along each arm (Fig. 1F).

Etymology. Named after the Greek mythological god of the dead and the king of the dark underworld, Hades, also husband of Persephone, akin to the habitat of the new asteroid species and to their co-existence; used as a noun in apposition.

Type locality. Clarion Clipperton Fracture Zone (IFREMER licence area), Eastern Pacific Ocean.

Distribution. Known only from the type locality (Fig. 4).

Habitat. The new species was collected from a wood fall among polymetallic fields in the Clarion Clipperton Fracture Zone. The specimen was collected with ROV *Kiel 6000* at 5030.7 m deep.

Colour pattern. Body colour in life is white (Fig. 5).

Remarks: Similarly to *C. persephone* nov. sp., the subpentagonal body shape of the new species, *C.hades* can be easily distinguished from *C. scrippscognaticausa* and *C. laguardai* having stellate body type (Fig. 1A vs. Shen et al.[22] Fig. 5A and Martin-Cao-Romero et al.[23] Fig. 1) as well as from *C. phorcynis* (Fig. 6) and *C. davidalani* (Shen et al.[22] Fig. 11 C) exhibiting also stellate body although less pronounced. The position of gonopores is similar to *C. persephone* and thus separating the new species from the species (*C. davidalani*, *C. scrippscognaticausa*, *C. spinimarginata*, *C.* cf. *spinimarginata*) having gonopores in notches on the proximal margin of two proximal-most superomarginal plates vs. piercing the supermarginal plates. As *C. persephone*, *C. hades*, concurs with the group of *Caymanostella* species that has granuliform abactinal armaments, which currently includes five of the ten *Caymanostella* species (*C. admiranda*, *C. hades*, *C. loresae*, *C. madagascarensis*, *C. persephone*). However, *C. hades* is clearly distinguished by its unique oval-shaped armaments, with a narrow base and crown with small multi-tipped prong-like support structures with multiple jagged tips (Fig. 3F, G and H). The two new species can be further discriminated by the terminal plate being square-shaped in *C. hades* (Fig. 2G) vs. being rectangular-shaped in *C. persephone* (Fig. 2C and D) and adambulacral spines in *C. hades* (Fig. 2K and L) are less serrated at tip than in *C. persephone* (Fig. 2I and J). Finally, the mean genetic p-distances between *C. hades* and its congeneric species ranged from 16.3 to 19.2% for COI, and 9.1–14.6% for 16S.

Phylogeny and genetic distances

The phylogenetic analysis (Fig. 7), conducted separately for COI and 16S genes and on a concatenated dataset (COI + 16 S + H3), identified both new species as distinct clades, clearly divergent from other known species and available caymanostellid sequences.

All three analyses strongly supported the monophyly of the *Caymanostella* genus (Fig. 7). Based on the concatenated dataset, two main clades were recovered within the genus, with one showing weak support. The well-supported clade includes the new species, *C. hades*, collected from the Clarion Clipperton Fracture Zone, and the *Caymanostella* species collected from the U.S.A. The mean genetic distance (p-distance) between the new species and its sister taxon, based on the 16S sequences, was 9.1% (Table 1).

The second clade includes the new species, *C. persephone*, along with the remaining six *Caymanostella* species collected from the Atlantic and Pacific Oceans. However, the phylogenetic relationships among these species and the new species were less resolved. The mean genetic distances between *C. persephone* and its congeneric species were significantly high, ranging from 13.3 to 18.2% for COI and 9.5–13.6% for 16S (Table 1). Notably, within this clade, the three Pacific species (*C. davidalani*, *C. scrippscognaticausa, C. cf. spinimarginata*), along with the Atlantic species *C. laguardai*, consistently formed a well-supported clade across all analyses (Fig. 7).

Discussion

Taxonomic assignment of the new species

Both morphological and molecular data support recognising two new species within the genus *Caymanostella*. The discovery increases the total number of known species in the genus to ten. It is highly likely that additional species remain undiscovered, as numerous *Caymanostella* records, particularly from the Southwest and Northeast Pacific as well as the Western Indian Ocean, have yet to be identified at species level. The phylogenetic tree topologies align with previous studies[21,22], and the monophyly of *Caymanostellidae* is further corroborated in the present study. However, due to the limited number of available *Caymanostella* sequences, particularly from the older described species, it is challenging to thoroughly evaluate the phylogenetic affinities between the new species and their congeners. The new species, although discovered on the same piece of sunken wood, are phylogenetically distinct, with a significant genetic distance separating them (Table 1). Similarly, the recently described species *C. davidalani* and *C. scrippscognaticausa* were also found in sympatry, sharing the same wood piece, yet exhibiting considerable genetic divergence. Despite this, these two species appear to have a closer phylogenetic relationship[22]. The newly discovered species, *Caymanostella persephone* nov. sp. and *C. hades* nov. sp., represent the first verified records of *Caymanostella* from the Clarion Clipperton Fracture Zone. Both species were collected from a single location on the same piece of sunken wood within the IFREMER licence area. Their presence was previously reported as cf. *Caymanostella* in photographs by Amon et al.[12] during their study of organic falls in the abyssal Clarion Clipperton Zone. The association of *Caymanostella* species with wood falls, combined with their rarity in the deep sea the species, makes encounters with these species infrequent[21,22]. Additionally, the ability to sample these species heavily depends on the type of sampling gear available during deep-sea expeditions, such as ROVs or dredges. Effective documentation of deep-sea biodiversity requires the use of diverse sampling methods[11]. The newly described species have only been reported as singletons from one locality to date. However, during sampling, they were observed in an aggregation (Fig. 5), although only two specimens could be collected.

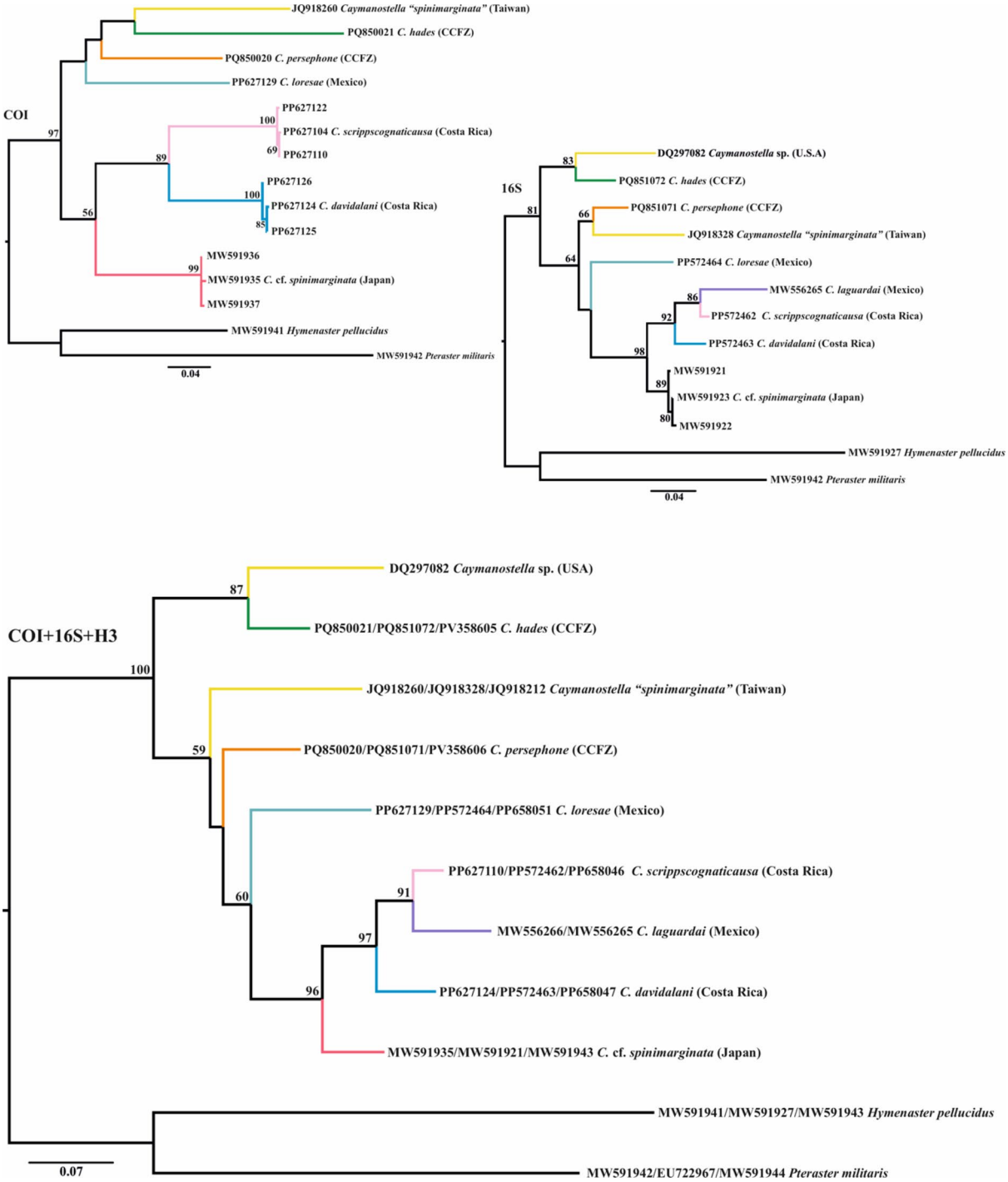

Fig. 7. Molecular phylogenetic tree based on the COI dataset, 16S dataset, and the concatenated dataset (COI + 16 S + H3) illustrating the relationships among members of *Caymanostella* and two outgroup taxa. Node values represent bootstrap support from the maximum likelihood analysis (RaxML). Bootstrap values ≥ 50% are shown. Colours correspond to the map depicted in Figure 4.

Global distribution of Caymanostella

The genus *Caymanostella* exhibits a fragmented distribution across tropical and temperate areas, with a known depth range spanning from 240 to 6780 m. Its actual distribution is likely far more extensive than currently documented. However, its association with a unique habitat —wood falls— and the extreme depths it occupies, which require specialised sampling equipment, contribute to its underrepresentation in the scientific literature. The newly described species represent some of the genus's deeper bathymetric records of the genus *Caymanostella* of 5030.7 m, surpassed only by the deepest record of *C. spinimarginata* (6740–6780 m) in the Cayman Trench, Caribbean Sea[24]. Among the ten species currently recognised within the genus including the new species, their

geographic distribution includes one species from the Atlantic Ocean (*C. spinimarginata*), one from the Indian Ocean (*C. madagascarensis*), two from the West Pacific (*C. admiranda*, *C. phorcynis*) and six from the East Pacific (*C. davidalani*, *C. hades* nov. sp., *C. laguardai*, *C. loresae*, *C. persephone* nov. sp., *C. scrippscognaticausa*) (Fig. 4; Supplementary Table S1).

Taxonomy and abyssal exploration

The abyssal plains including the Clarion-Clipperton Fracture Zone are among the world's most undersampled environments on Earth relative to their immense size[7]. Even for an area such as the Clarion Clipperton Zone proportion of undescribed species in the CCZ has been reported as being over 90% within taxa[9]. This staggering percentage highlights the vast biodiversity yet to be discovered in this region. Taxonomy, through detailed morphological descriptions and the collection of genetic data, is essential for understanding the life history of species such as *Caymanostella* and numerous other yet-to-be-described abyssal species. Such efforts will also enhance the identification of hard-to-study species, paving the way for mapping uncharted deep-sea ecosystems, their inhabitants, and the processes that enable life to thrive in these seemingly desolate environments. Especially in a potential area for mineral extraction, there is an urgent need for a better understanding of its unique ecosystem before any mining activities commence.

Methods

Material collection

The *Caymanostella* specimens were sampled from the Clarion Clipperton Fracture Zone in the Pacific Ocean during the cruise SO239, EcoResponse, with the Research Vessel Sonne in the framework of the European Joint Project Initiative – Ocean (JPI-O) Ecological Aspects of Deep-Sea Mining. Specimens were collected from IFREMER's licence for exploration area in station 161, 14° 2.07' N, 130° 5.60' W, on 15.04.2015 at depth 5030.7 m (Figs. 4 and 5) with a remotely operated vehicle (ROV *Kiel 6000*, GEOMAR) using the ROV's manipulator arm by direct picking. Both specimens were preserved in pre-cooled 96% EtOH. The ethanol was decanted after 24 h and replaced with new 96% EtOH to guarantee high ethanol concentration for preservation of high-quality DNA, and subsequently stored at −20 °C. In the laboratory at Senckenberg am Meer, Germany, an integrative molecular-morphological approach was implemented for the identification of the asteroid specimens. The type specimens are stored in the Senckenberg Research Institute and Natural History Museum Frankfurt (SMF).

Morphological species identification

A detailed morphological examination of the specimens collected was carried out. The holotypes were photographed in the lab using a Nikon D5 camera and stacked using the Helicon Focus. Several spines and spinelets/granules were taken from each holotype and mounted on aluminum stubs and palladium-coated for scanning electron microscopy (SEM, TESCAN VEGA 3XMU, Senckenberg am Meer) analysis. SEM analysis was performed after the different types of armature were cleaned in a mixture (1:1) of chlorinated bleach and distilled water. The scanned spines and spinelets/granules mounted on the stubs were deposited together with the type material at Senckenberg Research Institute and Natural History Museum Frankfurt (SMF). As each specimen represented a new species, a micro-CT was employed for a non-invasive approach. The specimens were imaged using the YXLON FF35 CT microcomputed tomography (microCT) system (equipped with a YXLON FXE Transmission Beam and Y.Panel 4343 CT Cs flat panel detector) of the Natural History Museum Vienna. An X-ray tube voltage of 120 kV and 130 kV, as well as a current of 400 µA was used. 3600 projection images were taken with an exposure time of 1 s each, and a 0.4 mm copper filter was utilized during scanning. The reconstructed isotropic voxel size ranged from 7.6 µm to 10.3 µm, depending on the overall specimen size. Volume renderings and virtual sections were visualized using Dragonfly 3D World 2024.1 software for Windows (Comet Technologies Canada Inc., Montreal, Canada). Finally, as no recent photos were available for the species *Caymanostella phorcynis* in the relevant literature digital photos were requested and provided by the Australian Museum (Fig. 6). All images were edited and compiled with CorelDRAW Graphics Suite v.26. The following abbreviations are used throughout this study: R, radius; r, inter-radius.

DNA extraction, amplification and sequencing

Genomic DNA extracted from the tube feet of the holotypes was used for genetic analyses. DNA extractions were carried out using the Monarch Nucleic Acid purification kit (New England Biolabs) following the manufacturer's guidelines. Two mitochondrial genes were targeted, cytochrome c oxidase subunit (COI) and 16S ribosomal RNA, along with a nuclear gene, Histone H3. DNA extractions were stored at −20 °C. A fragment of 658 bp, 527–528 bp, and 328 bp of the COI, 16S and H3 respectively were amplified by polymerase chain reaction (PCR). Amplifications were performed using AccuStart PCR SuperMix (ThermoFisher Scientific) in a 25-µL volume containing PCR SuperMix (9.5 µL ddH_2O, 12.5 µL AccuStart), 0.5 µL of each primer (10 pmol μL^{-1}) and 2 µL of DNA template. For the COI amplification, the forward primer LCOech1aF1 and the reverse primer jgHCO2198, tailed with M13F and M13R-pUC, respectively[25,26] were used. For the 16S gene, the primer pair 16Sar and 16Sbr[27] and the H3 gene, the primer pair H3F and H3R[28] were used and tailed as the COI primers. The amplification conditions consisted of an initial denaturation step of 3 min at 94 °C, 35 cycles of 30 s at 94 °C, 60 s at 47 °C, and 60 s at 72 °C, followed by a final extension step of 5 min at 72 °C. All PCR products were purified using ExoSap-IT (ThermoFisher Scientific). The amplified fragments were sequenced in both directions at Macrogen Europe Laboratory (Amsterdam, The Netherlands).

Phylogenetic analyses and genetic divergence

Forward and reverse sequences for each holotype were assembled and edited using Geneious v.9.1.7 (www.geneious.com[29]). Sequences were aligned with MAFFT v7.490 using the G-INS-i setting. Separate maximum

Species	Voucher	Locality	COI	16 S	H3	Reference
Caymanostella						
Caymanostella hades nov. sp.	SO239_161_2 (Holotype)	Clarion and the Clipperton Fracture Zone, (IFREMER licence area), Pacific Ocean	PQ850021	PQ851072	PV358605	Present study
Caymanostela persephone nov. sp.	SO239_161_1 (Holotype)	Clarion and the Clipperton Fracture Zone, (IFREMER licence area), Pacific Ocean	PQ850020	PQ851071	PV358604	Present study
Caymanostella davidalani Shen et al. 2024	SIO-BIC E7101 (Holotype)	Seamount 2, Costa Rica	PP627124	PP572463	PP658047	Shen et al. 2024
	MZUCR ECH2403 (Paratype)	Mound 12, Costa Rica	PP627125	--	--	
	SIO-BIC E7242	Jaco Scar, Costa Rica	PP627126	--	--	
Caymanostella laguardai Martin-Cao-Romero et al. (2021)	NHMUK:2021.1	Gulf of Mexico, Mexico	--	MW556266	MW556265	Martin-Cao-Romero et al. (2021)
Caymanostella loresae Shen et al. 2024	USNM1487403	Gulf of California, Mexico	PP627129	PP572464	PP658051	Shen et al. 2024
Caymanostella scrippscognaticausa Shen et al. 2024	SIO-BIC E11441 (Holotype)	Mound 11, Costa Rica	PP627110	PP572462	PP658046	Shen et al. 2024
	SIO-BIC E4403	Jaco Scar, Costa Rica	PP627104	--	--	
	SIO-BIC E4549E	Mound 12, Costa Rica	PP627122	--		
Caymanostella cf. *spinimarginata*	CsSO250-9-1	Kuril-Kamchatka Trench, Japan	MW591935	MW591921	MW591943	Dilman et al. (2022)
	CsSO250-9-2	Kuril-Kamchatka Trench, Japan	MW591936	MW591922	--	
	CsSO250-9-3	Kuril-Kamchatka Trench, Japan	MW591937	MW591923	--	
Caymanostella sp. ("*spinimarginata*")	MNHNP EcAh 5244	Taiwan	JQ918260	JQ918328	JQ918212	Foltz & Fatland (2012) unpublished
Caymanostella sp.	FMNH 5167	Oregon, USA	--	DQ297082	--	Janies et al. (2011)
Outgroup						
Hymenaster pellucidus Thomson, 1873	HpelPS128-44-1	Russia	MW591941	MW591927	MW591949	Dilman et al. (2022)
Pteraster militaris O.F. Müller, 1776	PtmilAMK54-4960-1/CASIZ 174,315	Russia	MW591942	EU722967	MW591950	Dilman et al. (2022)/Mah & Foltz (2011)

Table 2. Biogeographic information and GenBank accession numbers of specimens used in the present study for the phylogenetic analyses.

likelihood (ML) trees for the COI and the 16S genes, under the GTR + I + G and TIM3 + G models, respectively, as well as a concatenated tree (COI + 16S + H3), were constructed in RaxML-NG v.1.1.0[30] using the RaxML GUI v.2.0.10[31]. Optimal models were chosen with ModelTest-NG[32]. Ten ML searches were performed, and node support values were estimated using 1,000 bootstrap replicates under the thorough bootstrap method. The multi-loci (COI + 16S + H3) analysis was partitioned by gene and performed under the model GTR + G. The aligned concatenated dataset had a total of 2,318 nucleotide positions. The ML analyses were performed with the available data of the current dataset (Table 2) and supplemented with 11 additional COI and nine 16S and H3 Caymanostellidae sequences (Table 2) from the study of Martin-Cao-Romero et al.[23], Dilman et al.[21], and Shen et al.[22]. Two species of the Valavatida order in which the family Caymanostellidae belongs were used as outgroups (two COI, two 16S, two H3 sequences[21]; Table 2). Pairwise distances for COI and 16S sequences (Table 1) were computed with Mega X[33]. The sequences, trace files, collection data, and photos for each specimen are listed in the dataset CCZ_Caymanostella in BOLD (https://portal.boldsystems.org/recordset/DS-CCZ7). All sequences produced in the present study are deposited in GenBank, accession numbers of all sequences used, and specimen details can be found in Table 2.

Distribution records

Distribution records for all *Caymanostella* species (including *Caymanostella* spp.) were compiled from all accessible sources, both published and unpublished. This includes open collection data from various museums (see Supplementary Table S1), as well as the new records from the Clarion Clipperton Fracture Zone expedition. These compiled records are illustrated in Fig. 4. The map in Fig. 4 was generated using QGIS v.3.38[34] with raster map data from Natural Earth[35]. The map was then edited with CorelDRAW Graphics Suite v.26.

Data availability

The data presented in this study can be found beside the supplement in online repositories. GenBank, PQ851071-PQ851072, PQ850020- PQ850021 and PV358604-PV358605; Barcode of Life Database: https://portal.boldsystems.org/recordset/DS-CCZ7.

Received: 18 January 2025; Accepted: 30 April 2025
Published online: 21 May 2025

References

1. Hein, J. R., Koschinsky, A. & Kuhn, T. Deep-ocean polymetallic nodules as a resource for critical materials. *Nat. Rev. Earth Environ.* **1**, 158–169. https://doi.org/10.1038/s43017-020-0027-0 (2020).
2. Miller, K. A. et al. Challenging the need for deep seabed mining from the perspective of metal demand, biodiversity, ecosystems services, and benefit sharing. *Front. Mar. Sci.* **8**, 706161. https://doi.org/10.3389/fmars.2021.706161 (2021).
3. Hein, J. R. & Mizell, K. Chapter 8: Deep-Ocean Polymetallic Nodules and Cobalt-Rich Ferromanganese Crusts in the Global Ocean. In: *The United Nations Convention on the Law of the Sea, Part XI Regime and the International Seabed Authority: A Twenty-Five Year Journey* 177–197 (Brill, 2022).
4. Hein, J. R., Mizell, K., Koschinsky, A. & Conrad, T. A Deep-ocean mineral deposits as a source of critical metals for high- and green-technology applications: comparison with land-based resources. *Ore Geol. Rev.* **51**, 1–14. https://doi.org/10.1016/j.oregeorev.2012.12.001 (2013).
5. Lodge, M. et al. Seabed mining: international seabed authority environmental management plan for the Clarion-Clipperton zone. A partnership approach. *Mar. Policy*. **49**, 66–72. https://doi.org/10.1016/j.marpol.2014.04.006 (2014).
6. Wedding, L. M. et al. From principles to practice: a Spatial approach to systematic conservation planning in the deep sea. *P Roy Soc. Lond. B Bio*. **280**, 1684–1684. https://doi.org/10.1098/rspb.2013.1684 (2013).
7. Ramirez-Llodra, E. et al. Deep, diverse and definitely different: unique attributes of the world's largest ecosystem. *Biogeosciences* **7**, 2851–2899. https://doi.org/10.5194/bg-7-2851-2010 (2010).
8. Paulus, E. Shedding light on Deep-Sea Biodiversity—A highly vulnerable habitat in the face of anthropogenic change. *Front. Mar. Sci.* **8**, 667048. https://doi.org/10.3389/fmars.2021.667048 (2021).
9. Rabone, M. et al. How many metazoan species live in the world's largest mineral exploration region? *Curr. Biol.* **33**, 2383–2396. https://doi.org/10.1016/j.cub.2023.04.052 (2023).
10. Glover, A. G., Wiklund, H., Chen, C. & Dahlgren, T. G. Point of view: managing a sustainable deep-sea blue economy requires knowledge of what actually lives there. *eLife* **7**, e41319. https://doi.org/10.7554/eLife.41319 (2018).
11. Christodoulou, M. Unexpected high abyssal ophiuroid diversity in polymetallic nodule fields of the Northeast Pacific ocean and implications for conservation. *Biogeosciences* **17**, 1845–1876. https://doi.org/10.5194/bg-17-1845-2020 (2020).
12. Amon, D. et al. Insights into the abundance and diversity of abyssal megafauna in a polymetallic-nodule region in the Eastern Clarion-Clipperton zone. *Sci. Rep.* **6**, 30492. https://doi.org/10.1038/srep30492 (2016).
13. Simon-Lledó, E. et al. Multi-scale variations in invertebrate and fish megafauna in the mid-eastern Clarion Clipperton zone. *Prog Oceanogr.* **187**, e102405. https://doi.org/10.1016/j.pocean.2020.102405 (2020).
14. Uhlenkott, K., Meyn, K., Vink, A. & Martinez Arbizu, P. A review of megafauna diversity and abundance in an exploration area for polymetallic nodules in the Eastern part of the Clarion Clipperton fracture zone (North East Pacific), and implications for potential future deep-sea mining in this area. *Mar. Biodivers.* **53** https://doi.org/10.1007/s12526-022-01326-9 (2023).
15. Simon-Lledó, E. et al. Megafaunal variation in the abyssal landscape of the Clarion Clipperton zone. *Prog Oceanogr.* **170**, 119–133. https://doi.org/10.1016/j.pocean.2018.11.003 (2019).
16. Cuvelier, D. et al. Are seamounts refuge areas for fauna from polymetallic nodule fields? *Biogeosciences* **17**, 2657–2680. https://doi.org/10.5194/bg-17-2657-2020 (2020).
17. Uhlenkott, K., Simon-Lledó, E. & Vink, A. Martinez Arbizu, P. Investigating the benthic megafauna in the Eastern Clarion Clipperton fracture zone (north-east Pacific) based on distribution models predicted with random forest. *Sci. Rep.* **12**, 8229. https://doi.org/10.1038/s41598-022-12323-0 (2022).
18. Bribiesca-Contreras, G. et al. Benthic megafauna of the Western Clarion-Clipperton zone, Pacific ocean. *ZooKeys* **1113**, 1–110. https://doi.org/10.3897/zookeys.1113.82172 (2022).
19. Mah, C. L. & Blake, D. B. Global diversity and phylogeny of the Asteroidea (Echinodermata). *PLoS ONE*. **7**, e35644. https://doi.org/10.1371/journal.pone.0035644 (2012).
20. Rowe, F. W. E. A review of the family Caymanostellidae (Echinodermata: Asteroidea) with the description of a new species of Caymanostella Belyaev and a new genus. *Proc. Linn. Soc. N S W*. **111**, 293–307 (1989).
21. Dilman, A. B., Minin, K. V. & Petrov, N. B. New record of the wood-associated sea star *Caymanostella*, with notes on the phylogenetic position of the family Caymanostellidae (Asteroidea). *Zool. J. Linn. Soc.* **194**, 14–35. https://doi.org/10.1093/zoolinnean/zlab060 (2022).
22. Shen, Z., Mongiardino Koch, N., Seid, C. A., Tilic, E. & Rouse, G. W. Three new species of Deep-Sea Wood-Associated sea stars (Asteroidea: Caymanostellidae) from the Eastern Pacific. *Zootaxa* **5536**, 351–388. https://doi.org/10.11646/zootaxa.5536.3.1 (2024).
23. Martin-Cao-Romero, C., Solís-Marín, F. A. & Bribiesca-Contreras, G. *Crinitostella laguardai*, new genus and species of wood-dwelling deep-sea sea-star (Asteroidea: Caymanostellidae) from the Gulf of Mexico. *J. Mar. Biol. Assoc. U K.* **101**, 591–597. https://doi.org/10.1017/S0025315421000448 (2021).
24. Belyaev, G. M. A new family of abyssal starfishes. *Zool. Zhurnal.* **53**, 1502–1508 (1974).
25. Folmer, O. M., Black, W. & Hoen, R. DNA primers for amplification of mitochondrial cytochrome C oxidase subunit I from diverse metazoan invertebrates. *Mol. Mar. Biol. Biotech.* **3**, 294–299 (1994).
26. Layton, K. K. S., Corstorphine, E. A. & Hebert, P. D. N. Exploring Canadian echinoderm diversity through DNA barcodes. *PLoS ONE*. **11**, e0166118. https://doi.org/10.1371/journal.pone.0166118 (2016).
27. Simon, C. et al. Evolution, weighting, and phylogenetic utility of mitochondrial gene sequences and a compilation of conserved polymerase chain reaction primers. *Ann. Entomol. Soc. Am.* **87**, 651–701. https://doi.org/10.1093/aesa/87.6.651 (1994).
28. Colgan, D. J., Ponder, W. F., Beacham, E. & Macaranas, J. Gastropod phylogeny based on six segments from four genes representing coding or non-coding and mitochondrial or nuclear DNA. *Molluscan Res.* **23**, 123–148. https://doi.org/10.1071/MR03002 (2003).
29. Kearse, M. et al. Geneious basic: an integrated and extendable desktop software platform for the organization and analysis of sequence data. *Bioinformatics* **28**, 1647–1649. https://doi.org/10.1093/bioinformatics/bts199 (2012).
30. Kozlov, A. M., Darriba, D., Flouri, T., Morel, B. & Stamatakis, A. RAxML-NG: a fast, scalable and user-friendly tool for maximum likelihood phylogenetic inference. *Bioinformatics* **35**, 4453–4455. https://doi.org/10.1093/bioinformatics/btz305 (2019).
31. Edler, D., Klein, J., Antonelli, A. & Silvestro, D. RAxMLGUI 2.0: A graphical interface and toolkit for phylogenetic analyses using RAxML. *Methods Ecol. Evol.* **12**, 373–377. https://doi.org/10.1111/2041-210X.13512 (2020).
32. Darriba, D. et al. ModelTest-NG: A new and scalable tool for the selection of DNA and protein evolutionary models. *Mol. Biol. Evol.* **37**, 291–294. https://doi.org/10.1093/molbev/msz189 (2019).
33. Kumar, S., Stecher, G., Li, M., Knyaz, C. & Tamura, K. MEGA X: molecular evolutionary genetics analysis across computing platforms. *Mol. Biol. Evol.* **35**, 1547–1549. https://doi.org/10.1093/molbev/msy096 (2018).
34. QGIS Development Team. QGIS Geographic Information System, version 3.38. Open Source Geospatial Foundation http://qgis.org. (2024).
35. Natural Earth. Free vector and raster map data (2024). https://www.naturalearthdata.com

Acknowledgements
We thank Dr Claire Rowe, Mr Alex Hegedus and Dr Shane Ahyong (Australian Museum) for their help in acquiring the photos of Caymanostella phorcynis. Also thanks are due to Mrs Viola Winkler (Natural History Museum, Vienna) for her support and expertise in producing the micro-CT photos and Mrs Franczisca Iwan (Senckenberg am Meer). Finally, thanks are given to Mrs Nicol Mahnken (Senckenberg am Meer) and Agnes Bisenberger (Biodiversity Centre Upper Austria) for their expertise in acquiring the digital photos of the new species.

Author contributions
M.C. conceived the idea; P.M.A.: collected the samples. M.C., C.M., P.M.A.: designed the methodology; M.C. performed the lab work and collected the data; M.C., C.M., P.M.A.: data synthesis; M.C. aquired funding. M.C. led the writing of the manuscript. All authors reviewed and approved the submitted version of the manuscript.

Funding
This research was supported by the International Seabed Authority's Sustainable Seabed Knowledge Initiative: One Thousand Reasons Campaign (co-financed by the European Maritime and Fisheries Fund of the European Union, Project 101071214 – SSKI-I – EMFAF-2021-ISA-SSKI-IBA).

Declarations

Competing interests
The authors declare no competing interests.

Additional information
Supplementary Information The online version contains supplementary material available at https://doi.org/10.1038/s41598-025-00753-5.

Correspondence and requests for materials should be addressed to M.C.

Reprints and permissions information is available at www.nature.com/reprints.

Publisher's note Springer Nature remains neutral with regard to jurisdictional claims in published maps and institutional affiliations.